Revealing bosonic exchange symmetry in a two-photon temporal wave function

Yefeng Mei [1,*] Yue Jiang [2,*] and Shengwang Du [3,4,5,†]
[1]Department of Physics and Astronomy, Washington State University, Pullman, Washington 99164, USA
[2]Department of Physics and Astronomy, University of Pittsburgh, Pittsburgh, Pennsylvania 15260, USA
[3]Elmore Family School of Electrical and Computer Engineering, Purdue University, West Lafayette, Indiana 47907, USA
[4]Department of Physics and Astronomy, Purdue University, West Lafayette, Indiana 47907, USA
[5]Purdue Quantum Science and Engineering Institute, Purdue University, West Lafayette, Indiana 47907, USA

(Received 5 July 2025; accepted 22 December 2025; published 13 January 2026)

The wave function of two identical bosons remains invariant under particle exchange—a fundamental quantum symmetry that underlies Bose-Einstein statistics. We report the experimental observation of bosonic exchange symmetry in the temporal wave function of photon pairs generated via spontaneous four-wave mixing in a three-level cold atomic ensemble. The measured two-photon temporal correlations show excellent agreement with theoretical predictions based on symmetrized bosonic wave functions. In addition, we perform time-resolved two-photon interference to reconstruct the complex temporal wave function. Both the amplitude and phase profiles exhibit clear symmetry under photon exchange, providing a confirmation of bosonic exchange symmetry in the time domain.

DOI: 10.1103/sq4j-53jr

I. INTRODUCTION

In quantum mechanics, exchange symmetry is a fundamental principle governing the behavior of identical particles that constitute our universe. For fermions—such as electrons—exchanging two particles introduces a negative sign in their joint quantum state, reflecting their antisymmetric wave function, as illustrated in Fig. 1(a). In contrast, bosons obey a symmetric exchange rule: swapping their positions leaves the two-particle wave function unchanged [Fig. 1(b)]. These contrasting symmetries give rise to two distinct quantum statistics, Fermi-Dirac statistics for fermions and Bose-Einstein statistics for bosons, which underpin the structure of matter and the behavior of many-body quantum systems. Recently, theoretical advances have extended this classification beyond the fermion-boson dichotomy to include generalized and fractional (anyonic) statistics with nontrivial permutation phases [1,2], pointing to broader roles for exchange symmetry in topologically protected quantum computing and exotic quantum phases of matter [3–7].

Recent advances in the control and manipulation of individual quantum systems have made it possible to probe exchange symmetry in few-particle quantum states. For example, the Pauli exclusion principle has been experimentally confirmed via spin blockade spectroscopy in a double quantum dot system [8], where no two electrons can occupy the same quantum state. In the Hong-Ou-Mandel (HOM) interference experiment [9], two indistinguishable photons incident on a 50:50 beam splitter always exit the same output port due to bosonic exchange symmetry. Such bosonic bunching (or fermionic antibunching) has also been observed in ultracold atom experiments [10,11]. Although exchange-phase measurements have been demonstrated with photons [12–14] and proposed for trapped atoms or ions [15], a measurement of the symmetric (or antisymmetric) space-time complex wave function of two identical bosons (or fermions) remains an outstanding challenge. The definitive signature of exchange symmetry lies in the complex-valued joint wave function of the two-particle system, especially in the temporal domain, where symmetry under time-label exchange reveals intrinsic particle correlations and indistinguishability. Temporal and spectral degrees of freedom, in particular, offer a rich landscape for exploring novel symmetry-protected interference phenomena [16,17].

In this work, we report the observation of bosonic exchange symmetry in the temporal wave function of degenerate photon pairs generated from spontaneous four-wave mixing (SFWM) in a three-level laser-cooled ^{85}Rb atomic ensemble. The theory derived from symmetrized bosonic wave functions show excellent agreement with two-photon coincidence measurements. To gain deeper insight, we further perform two-photon interference to reconstruct the full complex temporal wave function. The observed amplitude and phase are invariant under photon exchange, revealing the manifestation of bosonic symmetry in the structure of the two-photon wave function.

II. EXPERIMENTAL SETUP

Figure 2 presents our experimental platform for generating and measuring correlated photon pairs. Cold ^{85}Rb atoms are loaded into a two-dimensional magneto-optical trap (MOT) with a length $L = 1.5$ cm and a temperature of about 10 μK [18]. After the MOT loading time, the atoms are optically

*These authors contributed equally to this work.
†Contact author: dusw@purdue.edu

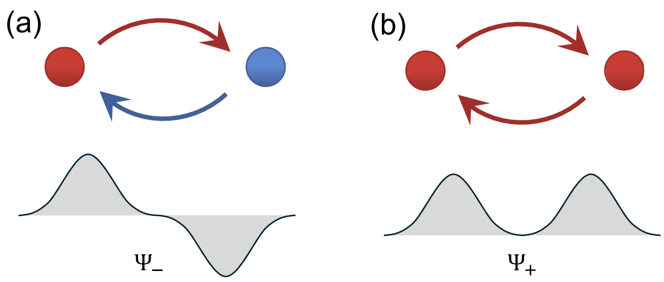

FIG. 1. Schematic illustration of exchange symmetry. Exchanging two undistinguishable particles leads to (a) antisymmetrized wave function Ψ_- for fermions, and (b) symmetrized wave function Ψ_+ for bosons.

pumped to the ground state $|1\rangle$, as depicted in the energy level diagram in Fig. 2(a). SFWM [19–22] is driven by a pair of pump (ω_p, 795 nm) and coupling (ω_c, 795 nm) laser beams, counterpropagating at an angle $\theta = 5^\circ$ with respect to the longitudinal z axis, as illustrated in Fig. 2(b). The pump is blue-detuned by Δ_p from the $|1\rangle \rightarrow |3\rangle$ transition, while the coupling laser is resonant with the $|2\rangle \rightarrow |3\rangle$ transition. The spontaneously generated and phase-matched Stokes (ω_s, $|3\rangle \rightarrow |2\rangle$) and anti-Stokes ($\omega_{as}$, $|3\rangle \rightarrow |1\rangle$) photons, moving backward along the z axis, are collected by two opposing single-mode fibers (SMFs) and detected by two single-photon counting modules (SPCMs 1 and 2: Excelitas SPCM-AQRH-16-FC). The two-photon coincidence is analyzed using a time-to-digital converter (Fast Comtec P7888). All optical fields are configured with the same circular polarization (σ^+). The hyperfine ground states $|1\rangle$ and $|2\rangle$ are separated by $\Delta_{12} = 2\pi \times 3.04$ GHz. Under phase-matching conditions, there are two equally weighted generation paths for each photon pair: (1) the Stokes photon is detected by SPCM 1 and the anti-Stokes photon by SPCM 2, and (2) the reverse detection configuration. By tuning the pump detuning to $\Delta_p = \Delta_{12}$, the Stokes and anti-Stokes photons become frequency degenerate ($\omega_{s0} = \omega_{as0} = \omega_0$) and thus indistinguishable, both experiencing the same linear propagation dispersion caused by electromagnetically induced transparency (EIT) [23,24]. As their spatial degrees of freedom are fixed (selected by the SMFs), in the following, we investigate the two-photon temporal wave function of these degenerate photon pairs. Our experimental setup also ensures the generated paired photons are indistinguishable in spectral and polarization modes.

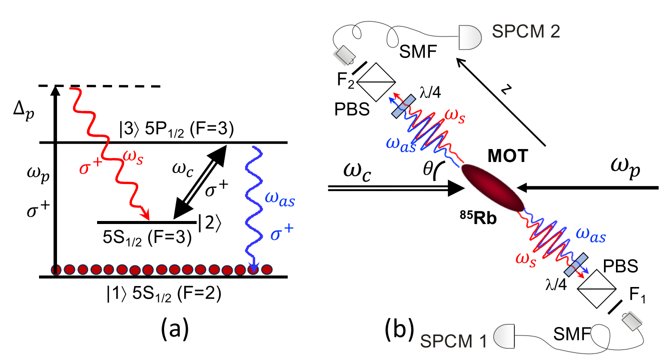

FIG. 2. Exchange symmetric photon-pair generation via spontaneous four-wave mixing (SFWM) in a laser-cooled ^{85}Rb atomic ensemble prepared in a magneto-optical trap (MOT). (a) Energy-level diagram of the three-level ^{85}Rb atomic system. (b) Schematic of the SFWM optical setup. $\lambda/4$: quarter-wave plate; PBS: polarizing beam splitter; $F_{1,2}$: narrow-band optical filters; SMF: single-mode fiber; SPCM: single-photon counting module.

III. THEORY OF TWO-PHOTON TEMPORAL WAVE FUNCTIONS WITH EXCHANGE SYMMETRIES

Assuming the Stokes and anti-Stokes photons can be labeled according to their respective atomic transitions, the degenerate two-photon temporal wave function can be expressed as [25,26]

$$\Psi(t_s, t_{as}) = \langle 0|\hat{a}_{as}(t_{as})\hat{a}_s(t_s)|\Psi\rangle = e^{-i\omega_0(t_s+t_{as})}\psi(\tau), \qquad (1)$$

where $|\Psi\rangle$ is the two-photon state, $\hat{a}_s$ and $\hat{a}_{as}$ are the photon annihilation operators, ω_0 is the central frequency, and $\tau = t_{as} - t_s$ is the relative delay between the photons arriving at their detectors. The relative two-photon temporal wave function $\psi(\tau)$ is given by

$$\psi(\tau) = \frac{L}{2\pi}\int d\varpi\, \kappa(\varpi)\Phi(\varpi)e^{-i\varpi\tau}, \qquad (2)$$

where $\varpi = \omega_{as} - \omega_0$ is the frequency detuning of the anti-Stokes photon. The nonlinear coupling coefficient is

$$\kappa(\varpi) = \frac{-i\Omega_p\Omega_c\gamma_{13}\mathrm{OD}\mu_{32}/(2\mu_{13}L)}{(\Delta_p + i\gamma_{13})[|\Omega_c|^2 - 4(\varpi + i\gamma_{13})(\varpi + i\gamma_{12})]}, \qquad (3)$$

where Ω_p and Ω_c are the Rabi frequencies of the pump and coupling lasers, respectively. OD is the optical depth for the $|1\rangle \rightarrow |3\rangle$ transition, μ_{mn} are dipole matrix elements, and L is the medium length. $\gamma_{13} = 2\pi \times 6$ MHz is the natural lifetime determined dephasing rate between $|1\rangle$ and $|3\rangle$. $\gamma_{12} = 2\pi \times 0.025$ MHz is the ground-state dephasing rate between $|1\rangle$ and $|2\rangle$. The phase-matching function $\Phi(\varpi)$ is given by

$$\Phi(\varpi) = \mathrm{sinc}\left[\frac{[k(\varpi) - k(-\varpi) + (k_p - k_c)]L}{2}\right] \times e^{i[k(\varpi)+k(-\varpi)]L/2}, \qquad (4)$$

where the wave number $k(\varpi) = k_0\sqrt{1 + \chi(\varpi)}$, with $k_0 = \omega_0/c$ and c being the speed of light in vacuum. Here, $k_p = \omega_p/c$ and $k_c = \omega_c/c$ are the pump and coupling laser wave numbers, respectively. The linear susceptibility under EIT conditions is

$$\chi(\varpi) = \frac{4\,\mathrm{OD}\,\gamma_{13}}{k_0 L}\frac{\varpi + i\gamma_{12}}{|\Omega_c|^2 - 4(\varpi + i\gamma_{13})(\varpi + i\gamma_{12})}. \qquad (5)$$

As discussed earlier, under perfect phase matching, there exist two indistinguishable and equally probable photon-pair generation paths: one where the Stokes photon is detected by SPCM 1 and the anti-Stokes photon by SPCM 2, and the other with the reverse detection configuration. Because the photons are indistinguishable, it is fundamentally impossible to assign a Stokes or anti-Stokes label at the detectors. To account for exchange symmetry, we consider the symmetrized (bosonic) and antisymmetrized (fermionic) two-photon wave functions at the detectors, given by

$$\Psi_\pm(t_1, t_2) = e^{-i\omega_0(t_1+t_2)}[\psi(\tau) \pm \psi(-\tau)], \qquad (6)$$

where $\tau = t_2 - t_1$, and the "+" and "−" signs correspond to bosonic and fermionic exchange symmetry, respectively.

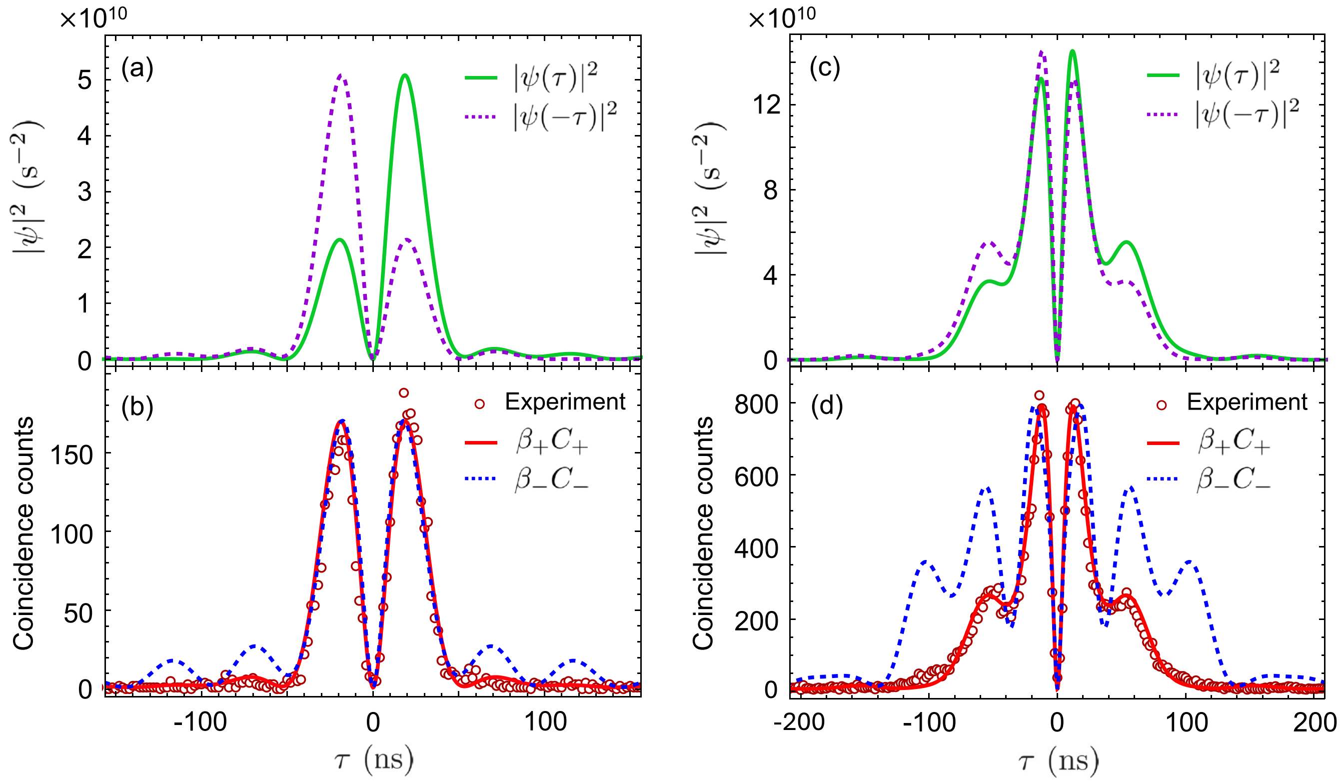

FIG. 3. Two-photon temporal wave functions at different optical depths (OD). (a), (b) OD = 7; (c), (d) OD = 25. (a), (c) Theoretical temporal wave functions $\psi(\tau)$ and $\psi(-\tau)$ of Stokes–anti-Stokes photon pairs. (b), (d) Measured two-photon coincidence counts (red circles), compared with theoretical predictions $\beta_\pm C_\pm(\tau)$ based on symmetrized (bosonic, +, red solid line) and antisymmetrized (fermionic, −, blue dashed line) wave functions. Other experiment parameters are $\Omega_p = 2\pi \times 88.8$ MHz and $\Omega_c = 2\pi \times 20.7$ MHz.

Let ξ denote the duty cycle, η the joint detection efficiency (including fiber coupling efficiency, filter transmissions, and detector efficiencies), T the total data acquisition time, and δt the time-bin width of the SPCMs. The two-photon coincidence counts are then given by

$$C_\pm(\tau) = \xi\eta T\delta t\,|\Psi_\pm(t_1, t_2)|^2 = \xi\eta T\delta t\,|\psi(\tau) \pm \psi(-\tau)|^2. \tag{7}$$

In our experimental setup, the parameters are $\eta = 0.05$, $T = 1200$ s, $\delta t = 2$ ns, with $\xi = 1.5\%$ for OD = 7 and $\xi = 1.2\%$ for OD = 25. In the following, we investigate how this temporal coincidence measurement reflects the bosonic nature of photons.

IV. WAVEFORM COMPARISON BETWEEN THEORY AND EXPERIMENT

Figure 3 presents both theoretical and experimental results for different optical depths (OD). At OD = 7 [Fig. 3(a)], the temporal wave function $\psi(\tau)$ is neither symmetric [$\psi(\tau) = \psi(-\tau)$] nor antisymmetric [$\psi(\tau) = -\psi(-\tau)$], yet there exists a substantial overlap between $\psi(\tau)$ and $\psi(-\tau)$. This partial overlap leads to pronounced interference effects in the two-photon correlations, depending on whether bosonic or fermionic exchange symmetry is applied, as described by Eqs. (6) and (7). In Fig. 3(b), we compare the experimentally measured two-photon coincidence counts with theoretical predictions $\beta_\pm C_\pm(\tau)$, where $\beta_\pm$ are vertical scaling factors optimized to best fit the data. The symmetrized (bosonic) result, $\beta_+C_+(\tau)$, shows excellent agreement with the experimental measurements. In contrast, the antisymmetrized (fermionic) prediction, $\beta_-C_-(\tau)$, deviates significantly, particularly in the form of oscillatory features at $|\tau| > 50$ ns, which are not observed experimentally. The fitted scaling factor $\beta_+ = 0.7$ for the symmetrized case indicates great agreement with the measured coincidences in amplitude, close to the ideal value of 1 where the discrepancy may arise from the system loss. In contrast, the antisymmetrized prediction requires a notably larger scaling factor, $\beta_- = 16.5$, to match the data range. This mismatch grows even more pronounced at OD = 25. As shown in Fig. 3(c), the overlap between $\psi(\tau)$ and $\psi(-\tau)$ increases, enhancing the sensitivity to exchange symmetry. Figure 3(d) again compares the experimental data with theory, showing that the bosonic prediction $\beta_+C_+(\tau)$ (with $\beta_+ = 1.0$) closely matches the measurement, while the fermionic model $\beta_-C_-(\tau)$ requires an unphysical scaling factor of $\beta_- = 179.5$ to approximate the measured coincidence level. The large β_- values clearly reflect the incompatibility between the antisymmetric (fermionic) wave function and experimental observations.

To quantitatively determine agreement between the theory and experimentally measured waveforms, we compute the waveform fidelities $F_\pm$, defined as

$$F_\pm = \frac{|\int d\tau\,\sqrt{C_\pm(\tau)}\,\sqrt{C_{\rm expt}(\tau)}|^2}{[\int d\tau\,C_\pm(\tau)][\int d\tau\,C_{\rm expt}(\tau)]}, \tag{8}$$

where $C_{\rm expt}(\tau)$ is the experimentally measured coincidence counts. We obtain $F_+ = 96.87\% > F_- = 88.75\%$ for OD =

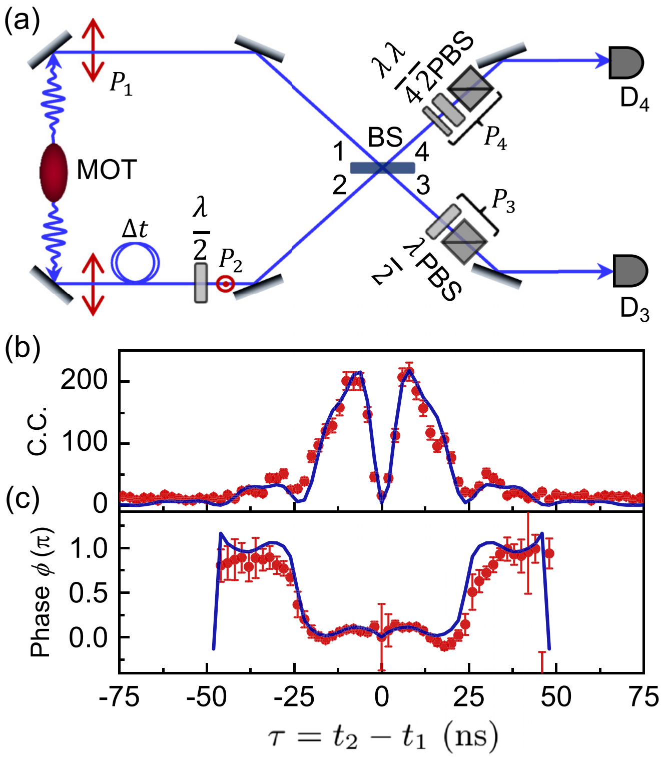

FIG. 4. Measurement of the complex temporal wave function of degenerate photon pairs using time-resolved two-photon interference. (a) Experimental setup for reconstructing the two-photon complex temporal wave function generated via backward SFWM. (b) Two-photon coincidence counts (C.C.) measured before the beam splitter (BS), representing the squared amplitude of the temporal wave function. (c) Reconstructed phase profile of the two-photon temporal wave function. The solid lines in (b) and (c) are theoretical plots.

7, and $F_+ = 99.23\% > F_- = 88.09\%$ for OD = 25. Both the correlation profiles (measured by $F_\pm$) and fitted scaling factors ($\beta_\pm$) support the conclusion that the experimentally measured two-photon temporal wave functions obey bosonic exchange symmetry.

V. EXCHANGE SYMMETRY IN PHASE AND AMPLITUDE

To unambiguously verify bosonic exchange symmetry, we measure the phase profile of the two-photon temporal wave function using time-resolved two-photon interference [27]. As illustrated in Fig. 4(a), the initially circularly polarized, counterpropagating photon pairs are converted into linearly polarized modes via quarter-wave ($\lambda/4$) plates and then coupled into polarization-maintaining (PM) SMFs. The fiber outputs are set to orthogonal polarizations: horizontal (P_1, ↔) and vertical (P_2, ↕), with P_2 rotated by a half-wave ($\lambda/2$) plate. The relative (optical) time delay Δt between the two paths can be varied by setting the length difference of the PM SMFs. The photons are subsequently combined at a 50:50 beam splitter (BS), whose output ports (3 and 4) pass through polarizers P_3 and P_4 and are detected by two SPCMs (D_3 and D_4). Polarizer P_3 consists of a half-wave plate followed by a polarizing beam splitter (PBS), while P_4 includes a quarter-wave plate, a half-wave plate, and a PBS. Further experimental details are provided in Ref. [27]. The amplitude profile of the two-photon wave function is obtained from the coincidence counts measured before the BS [Fig. 4(b)]. To reconstruct the phase, we collect 12 sets of coincidence measurements under different combinations of polarization projections (P_3 and P_4) at a distinct relative delay $\Delta t = 1.0$ ns. The extracted phase profile $\phi(\tau)$ is shown in Fig. 4(c). With the measured amplitude and phase, we can define and compute the state fidelity as follows,

$$F = \frac{|\int d\tau\, \Psi^*_{\rm th}(\tau)\Psi_{\rm expt}(\tau)|^2}{[\int d\tau |\Psi_{\rm th}(\tau)|^2][\int d\tau |\Psi_{\rm expt}(\tau)|^2]}, \quad (9)$$

where $\Psi_{\rm th}(\tau)$ and $\Psi_{\rm expt}(\tau)$ are the theoretically predicted and experimentally reconstructed biphoton complex wave functions. We obtain the state fidelity to be $F = 97.02\%$. The observed symmetry in both the amplitude and phase functions confirms that the temporal wave function of the two indistinguishable photons exhibits bosonic exchange symmetry.

VI. CONCLUSION

In summary, we have observed bosonic exchange symmetry in the temporal wave function of indistinguishable photon pairs generated via SFWM from a cold atomic ensemble. By measuring two-photon temporal correlations at varying optical depths, we confirmed that the experimental coincidence profiles agree with symmetrized theoretical predictions and are inconsistent with antisymmetric alternatives. Furthermore, through time-resolved two-photon interference, we reconstructed both the amplitude and phase of the complex temporal wave function and verified its exchange symmetry. These results provide a time-domain confirmation of bosonic exchange symmetry and offer an alternative route toward probing fundamental quantum physics in few-particle systems. We note that any residual distinguishability between the paired photons can influence the measured temporal wavefunction. For example, a slight spectral mismatch introduces a time-dependent relative phase in the two-photon wave function, and imperfect polarization matching degrades the two-photon interference measurements for phase reconstruction. Consequently, we carefully optimize the alignment of the experimental setup to ensure that the generated photon pairs are indistinguishable in their spectral and polarization modes. The small discrepancies observed between theory and experiment are likely attributable to these residual imperfections in indistinguishability.

ACKNOWLEDGMENTS

S.D. acknowledges the support from NSF (Grants No. 2500662 and No. 2228725) and DOE (DE-SC0022069). Y.J. acknowledges the support from the PQI community award. Y.M. acknowledges the support from the WSU New Faculty Seed Grant.

DATA AVAILABILITY

The data that support the findings of this article are openly available [28], embargo periods may apply.

[1] Z. Wang and K. R. A. Hazzard, Particle exchange statistics beyond fermions and bosons, Nature (London) **637**, 314 (2025).
[2] M. C. Tichy and K. Mølmer, Extending exchange symmetry beyond bosons and fermions, Phys. Rev. A **96**, 022119 (2017).
[3] R. Stárek, M. Mičuda, M. Miková, I. Straka, M. Dušek, P. Marek, M. Ježek, R. Filip, and J. Fiurášek, Nondestructive detector for exchange symmetry of photonic qubits, npj Quantum Inf. **4**, 35 (2018).
[4] S. Coen, B. Garbin, G. Xu, L. Quinn, N. Goldman, G.-L. Oppo, M. Erkintalo, S. G. Murdoch, and J. Fatome, Nonlinear topological symmetry protection in a dissipative system, Nat. Commun. **15**, 1398 (2024).
[5] J. Boeyens, B. Yadin, and S. Nimmrichter, How exchange symmetry impacts performance of collective quantum heat engines, New J. Phys. **27**, 013021 (2025).
[6] S. Musolino, M. Albert, A. Minguzzi, and P. Vignolo, Symmetry oscillations in strongly interacting one-dimensional mixtures, Phys. Rev. Lett. **133**, 183402 (2024).
[7] H.-T. Lim, J.-C. Lee, K.-H. Hong, and Y.-H. Kim, Observation of decoherence-induced exchange symmetry breaking in an entangled state, Phys. Rev. A **90**, 052328 (2014).
[8] K. Ono, D. G. Austing, Y. Tokura, and S. Tarucha, Current rectification by Pauli exclusion in a weakly coupled double quantum dot system, Science **297**, 1313 (2002).
[9] C. K. Hong, Z. Y. Ou, and L. Mandel, Measurement of subpicosecond time intervals between two photons by interference, Phys. Rev. Lett. **59**, 2044 (1987).
[10] T. Jeltes, J. M. McNamara, W. Hogervorst, W. Vassen, V. Krachmalnicoff, M. Schellekens, A. Perrin, H. Chang, D. Boiron, A. Aspect, and C. I. Westbrook, Comparison of the hanbury brown–twiss effect for bosons and fermions, Nature (London) **445**, 402 (2007).
[11] A. M. Kaufman, M. C. Tichy, F. Mintert, A. M. Rey, and C. A. Regal, The Hong–Ou–Mandel effect with atoms, in *Advances in Atomic, Molecular, and Optical Physics*, edited by E. Arimondo, L. F. DiMauro, and S. F. Yelin (Academic, San Diego, 2018), Vol. 67 Chap. 7, pp. 377–427.
[12] K. Tschernig, C. Müller, M. Smoor, T. Kroh, J. Wolters, O. Benson, K. Busch, and A. Perez-Leija, Direct observation of the particle exchange phase of photons, Nat. Photon. **15**, 671 (2021).
[13] Y. Wang, M. Piccolini, Z.-Y. Hao, Z.-H. Liu, K. Sun, J.-S. Xu, C.-F. Li, G.-C. Guo, R. Morandotti, G. Compagno, and R. L. Franco, Proof-of-principle direct measurement of particle statistical phase, Phys. Rev. Appl. **18**, 064024 (2022).
[14] Z.-F. Liu, C. Chen, J.-M. Xu, Z.-M. Cheng, Z.-C. Ren, B.-W. Dong, Y.-C. Lou, Y.-X. Yang, S.-T. Xue, Z.-H. Liu, W.-Z. Zhu, X.-L. Wang, and H.-T. Wang, Hong-Ou-Mandel interference between two hyperentangled photons enables observation of symmetric and antisymmetric particle exchange phases, Phys. Rev. Lett. **129**, 263602 (2022).
[15] C. F. Roos, A. Alberti, D. Meschede, P. Hauke, and H. Häffner, Revealing quantum statistics with a pair of distant atoms, Phys. Rev. Lett. **119**, 160401 (2017).
[16] V. V. Orre, E. A. Goldschmidt, A. Deshpande, A. V. Gorshkov, V. Tamma, M. Hafezi, and S. Mittal, Interference of temporally distinguishable photons using frequency-resolved detection, Phys. Rev. Lett. **123**, 123603 (2019).
[17] N. J. Cerf and M. G. Jabbour, Two-boson quantum interference in time, Proc. Natl. Acad. Sci. USA **117**, 33107 (2020).
[18] S. Zhang, J. F. Chen, C. Liu, S. Zhou, M. M. T. Loy, G. K. L. Wong, and S. Du, A dark-line two-dimensional magneto-optical trap of ^{85}Rb atoms with high optical depth, Rev. Sci. Instrum. **83**, 073102 (2012).
[19] L. Zhao, X. Guo, C. Liu, Y. Sun, M. M. T. Loy, and S. Du, Photon pairs with coherence time exceeding one microsecond, Optica **1**, 84 (2014).
[20] Y. Mei, Y. Zhou, S. Zhang, J. Li, K. Liao, H. Yan, S.-L. Zhu, and S. Du, Einstein-Podolsky-Rosen energy-time entanglement of narrow-band biphotons, Phys. Rev. Lett. **124**, 010509 (2020).
[21] X. Guo, Y. Mei, and S. Du, Testing the bell inequality on frequency-bin entangled photon pairs using time-resolved detection, Optica **4**, 388 (2017).
[22] S. Du, P. Kolchin, C. Belthangady, G. Y. Yin, and S. E. Harris, Subnatural linewidth biphotons with controllable temporal length, Phys. Rev. Lett. **100**, 183603 (2008).
[23] S. E. Harris, Electromagnetically induced transparency, Phys. Today **50**(7), 36 (1997).
[24] M. Fleischhauer, A. Imamoglu, and J. P. Marangos, Electromagnetically induced transparency: Optics in coherent media, Rev. Mod. Phys. **77**, 633 (2005).
[25] S. Du, J. Wen, and M. H. Rubin, Narrowband biphoton generation near atomic resonance, J. Opt. Soc. Am. B **25**, C98 (2008).
[26] X. Lai, C. Li, A. Zanders, Y. Mei, and S. Du, Symmetry protected two-photon coherence time, Phys. Rev. Lett. **133**, 033601 (2024).
[27] P. Chen, C. Shu, X. Guo, M. M. T. Loy, and S. Du, Measuring the biphoton temporal wave function with polarization-dependent and time-resolved two-photon interference, Phys. Rev. Lett. **114**, 010401 (2015).
[28] Y. Jiang, Y. Mei, and S. Du, Revealing bosonic exchange symmetry in two-photon temporal wavefunction (Version v1) [Data set], Zenodo (2025), https://doi.org/10.5281/zenodo.17860885.